

Preparation of FeAPO-5 Molecular Sieve Thin Films and Application as a Capacitive Type Humidity Sensor

Trinidad Muñoz, Jr. and Kenneth J. Balkus, Jr.*

Department of Chemistry, University of Texas at Dallas, Richardson, Texas 75083-0688

Received July 22, 1998. Revised Manuscript Received October 6, 1998

Thin films of FeAPO-5 molecular sieves deposited on TiN-coated silicon wafers have been generated using pulsed laser ablation. The FeAPO-5 films were employed as the dielectric phase in a capacitive type chemical sensor. The FeAPO-5-based sensors exhibited significant changes in capacitance upon exposure to moisture. Interestingly, the sensor also responded to moisture from breathing which makes it useful not only as a potential humidity sensor but as a respiration monitoring device.

Introduction

Molecular sieves constitute a class of low-density crystalline metal oxides that are composed of one-, two-, and three-dimensional pores and/or cage structures.¹ The size and shape of the pores allow these materials to be discriminating in the adsorption of small molecules. These characteristics make molecular sieves attractive materials for selective chemical sensors. Zeolite molecular sieves have been employed in a variety of chemical sensors where the transduction mechanism involves changes in mass, optical properties, and capacitance, as shown in Table 1. For example, some of the more widely studied sensor configurations that employ molecular sieves include surface acoustic wave (SAW) and quartz crystal mass (QCM) sensors. The SAW and QCM devices essentially respond to the weight change in a zeolite coating upon absorption of small molecules. Such zeolite-based chemical sensors have shown promise for the detection of volatile organics, as shown in Table 1. However these mass sensitive devices are less discriminating with smaller gases such as N₂, O₂, and CO₂. Zeolites modified with ions or molecules that register an optical change upon exposure to certain analytes can be quite selective. However the range of molecules that can be detected as well as the reversibility and thermal stability of optical zeolite sensors are limited.

A capacitive type chemical sensor employs the molecular sieve as the dielectric phase between two electrodes, whereupon adsorption of an analyte the capacitance changes. An attractive feature of these sensors is the fact that not only are the size and shape selectivity operative but molecules of different polarity should also elicit different sensor responses. Another advantage of using capacitive type sensors is the simple device configuration which can easily be microfabricated and combined with other similar sensors in an array format. Most of the molecular sieve sensors of this variety in Table 1 have been fabricated in a parallel plate configuration which requires a thin continuous film. This is

because capacitance is inversely proportional to the distance between the electrodes ($C = A\epsilon/d$), where A is the area of the electrode, ϵ is the permittivity in a vacuum, and d is the distance between the electrodes. Additionally, the molecular sieve film must be continuous to prevent a short circuit between the parallel plate electrodes. We have shown that pulsed laser ablation is an effective technique for the preparation of continuous and sometimes oriented molecular sieve thin films.^{2–6} The versatile nature of this method allows one to prepare well-adhered submicron thin molecular sieve films on substrates such as silicon, platinum, tantalum, titanium nitride (TiN), indium-doped tin oxide (ITO) glass, and Mylar. Pulsed laser deposition (PLD) involves a high-intensity excimer laser (e.g., KrF*, 248 nm) that is used to irradiate a molecular sieve target and generate a plume of particles onto a temperature-controlled substrate.

The thin films of aluminum phosphate (AlPO₄) and metal-substituted molecular sieves (MeAPO, Me = Co, Fe, V, Mg, Mn) listed in Table 1 were prepared by laser ablation and fabricated into capacitive type chemical sensors.^{2–9} These molecular sieve based sensors exhibited varying responses to gases such as N₂, CO, CO₂, H₂O, and NH₃ which appear to depend on the lattice composition and pore structure. Since different molecular sieves have different signature responses to certain molecules, the fabrication of an array that could be used to identify gases may eventually be possible. As part of a continuing study of different MeAPO molecular

(2) Balkus, K. J., Jr.; Riley, S. J.; Gnade, B. E. *Mater. Res. Soc. Symp. Proc.* **1994**, *351*, 437.

(3) Balkus, K. J., Jr.; Sottile, L.; Riley, S. J.; Gnade, B. E. *Thin Solid Films* **1995**, *260*, 4.

(4) Sottile, L.; Balkus, K. J., Jr.; Riley, S. J.; Gnade, B. E. *Mater. Res. Soc. Symp. Proc.* **1994**, *351*, 263.

(5) Balkus, K. J., Jr.; Sottile, L. J.; Nguyen, H.; Riley, S. J.; Gnade, B. E. *Mater. Res. Soc. Symp. Proc.* **1995**, *371*, 33.

(6) Balkus, K. J., Jr.; Ball, L. J.; Gnade, B. E.; Anthony, J. M. *Chem. Mater.* **1997**, *9*, 380.

(7) Balkus, K. J., Jr.; Ball, L. J.; Gimon-Kinsel, M. E.; Anthony, J. M.; Gnade, B. E. *Sensors Actuators B* **1997**, *42*, 67.

(8) Ball, L. J., D. Chem. Dissertation University of Texas at Dallas, **1996**.

(9) Gimon-Kinsel, M. E.; Balkus, K. J., Jr. Manuscript in preparation.

(1) Szostak, R. *Molecular Sieves*, 2nd ed.; Thomas Science: Springfield, IL, 1998.

Table 1. Molecular Sieve Chemical Sensors

molecular sieve	analytes	refs
Capacitive		
parallel plate		
AlPO ₄ -5, -H3, -H1	CO ₂ , CO, N ₂ , H ₂ O, toluene	2-6
MeAPO-5 (Me = Mn, V, Co, Fe)	CO ₂ , CO, N ₂ , NH ₃ , H ₂ O	6-8
MAPO-36	CO ₂ , CO, N ₂ , H ₂ O	7
Nb-TMS-1	methanol, acetone, H ₂ O	9
Interdigital		
NaY	C ₄ H ₁₀ , CO, H ₂ , H ₂ O, NO, NH ₃ , O ₂ , butane	10-14
NaX	butane	10
Impedance		
NaY	butane, H ₂ O, NH ₃ , NO	12
Surface Acoustic Wave		
NaY	C ₄ H ₁₀ , CO, H ₂ , H ₂ O, NO, NH ₃ , O ₂ , methanol, ethanol, CH ₃ Cl, chloroform, CCl ₄ , isooctane	15,16
NaA	chloroform, CCl ₄ , pentane, isooctane, H ₂ O, ethanol, methanol, CH ₃ Cl, toluene, butanol, hexane	15,16
ZSM-5	methanol, propanol, isooctane, pyridine	
MCM-41	aromatics, CO, CO ₂ , NH ₃ , NO _x , HCN, enzymes	17
chabazite	NH ₃ , tributylamine	15,16
CuY	NH ₃ , pyridine	15,16
Quartz Crystal Microbalance		
silicalite	ethanol, H ₂ O, methanol, CH ₃ Cl, chloroform, CCl ₄ , isooctane	18
NaY	C ₄ H ₁₀ , CO, H ₂ , H ₂ O, NO, NH ₃ , O ₂ , methanol, ethanol, CH ₃ Cl, chloroform, CCl ₄ , isooctane	18
NaA	chloroform, CCl ₄ , pentane, isooctane, H ₂ O, ethanol, methanol, CH ₃ Cl, toluene, butanol, hexane	18
Optical		
Cu-ZSM-5	O ₂	19
MCM-41	aromatics, CO, CO ₂ , NH ₃ , NO _x , HCN, enzymes, glycoproteins	17
NaY/Ru-dipy	C ₄ H ₁₀ , CO, H ₂ , H ₂ O, NO, NH ₃ , O ₂ , methanol, ethanol, CH ₃ Cl, chloroform, CCl ₄ , isooctane	20
NaY/Eu ³⁺	O ₂	21
NaY/Ti(IV)O _x	H ₂ , O ₂	22
sodalite	NO ₂	23, 24
MnAPSO-44	N ₂ O, CO, N ₂ , O ₂	23

sieves for this application, the results for pulsed laser deposition of an iron-substituted aluminum phosphate (FeAPO-5) is described below. The FeAPO-5 molecular sieve has the AFI topology and consists of a one-dimensional channel structure running in parallel with a pore diameter of 7.3 Å, as shown in Figure 1.²⁵ A capacitance type sensor based on the laser-deposited

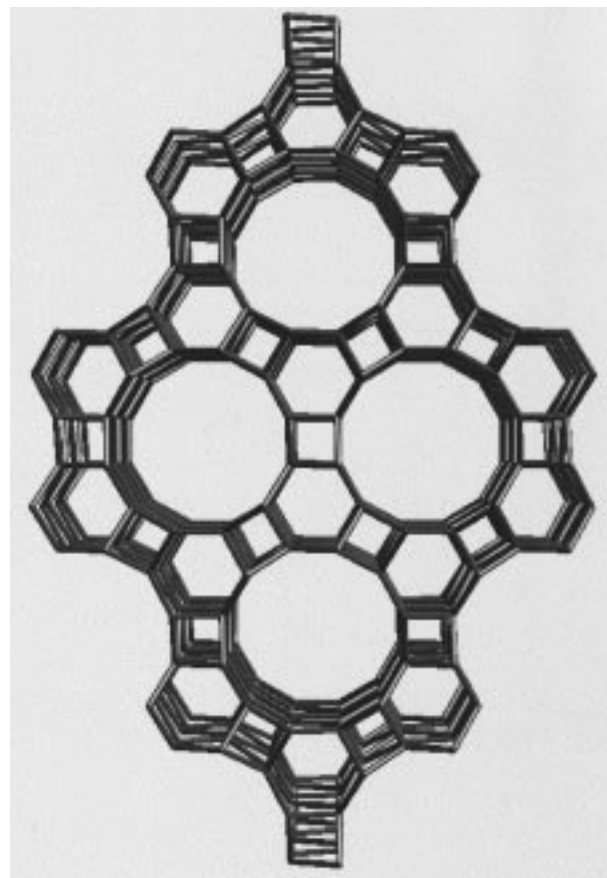


Figure 1. Framework structure of FeAPO-5 viewed along the 100 direction (oxygen atoms have been omitted for clarity) calculated using the crystallographic data in ref 25.

FeAPO-5 films has been shown to be particularly sensitive to moisture. These results as well as the preparation and characterization of the FeAPO-5-based chemical sensor are described below.

Experimental Section

Materials. FeAPO-5 was synthesized according to the literature procedure²⁶ by first combining 1.0 g of FeCl₂·4H₂O (Aldrich) with 3.5 mL of 85% H₃PO₄ (Fisher) in 9.1 mL of deionized H₂O. Then 3.1 g of Al(OH)₃ (Pfalz and Bauer) were added to the iron phosphoric acid solution and stirred at room temperature for ~5 min. The FeAPO-5 gel was then combined with 9.2 mL of 40% tetraethylammonium hydroxide (Alpha) and stirred until homogeneous (pH ~3). The gel was then transferred into a 20 mL PTFE-lined autoclave (Parr) and heated under static conditions at 150 °C for 18 h. The resulting blue-gray FeAPO-5 crystals were washed with deionized water and isolated by centrifugation. The as synthesized FeAPO-5 material was found to have a unit cell composition of [Fe_{0.8}Al_{11.3}P₁₂O₄₈] as determined by elemental analysis

(10) Alberti, K.; Haas, J.; Plog, C.; Fetting, F. *Catal. Today* **1997**, *8*, 509.

(11) Alberti, K.; Fetting, F. *Sensors Actuators B* **1994**, *21*, 39.

(12) Plog, C.; Maunz, W.; Kurzweil, P.; Obermeier, E.; Scheibe, C. *Sensors Actuators B* **1995**, *24-25*, 403.

(13) Kurzweil, P.; Maunz, W.; Plog, C. *Sensors Actuators B* **1995**, *24-25*, 653.

(14) Mercer, W. C.; Coughlin, P. K.; McLeod, D., Jr.; Flanigen, E. M. U. S. Patent 4,860,584, 1989.

(15) Bein, T.; Brown, K. *J. Am. Chem. Soc.* **1989**, *111*, 7640.

(16) Bein, T.; Brown, K. D.; Frye, G. C.; Brinker, C. J. U.S. Patent 5,151,110, 1992.

(17) Olson, D. H.; Stucky, G. D.; Vartuli, J. C. U.S. Patent 5,364,797, 1994.

(18) Yan, Y.; Bein, T. *J. Phys. Chem.* **1992**, *96*, 9387.

(19) Weber, W. H.; Poindexter, B. D.; Remillard, J. T. U.S. Patent 5,490,490, 1996.

(20) Meier, B.; Werner, T.; Klimant, I.; Wolfbeis, O. S. *Sensors Actuators B* **1995**, *29*, 240.

(21) Baker, M. D.; Olken, M. M.; Ozin, G. A. *J. Am. Chem. Soc.* **1998**, *110*, 5709.

(22) Grubert, G.; Wark, M.; Jaeger, N. I.; Schulz-Ekloff, G.; Tkanchenko, O. P. *J. Phys. Chem B* **1998**, *102*, 1665.

(23) Ozin, G. A.; Kuperman, A.; Stein, A. *Angew. Chem., Int. Ed. Engl.* **1989**, *28*, 359.

(24) Jiang, M. R. M.; Weller, M. T. *Sensors. Actuators B* **1996**, *30*, 3.

(25) Mora, A. J.; Fitch, A. N.; Cole, M.; Goyal, R.; Jones, R. H.; Jobic, H.; Carr, S. W. *J. Mater. Chem.* **1996**, *11*, 1831.

(26) Messina, C. A.; Lok, B. M.; Flanigen, E. M. U. S. Patent 4,554,143, 1985.

(Galbraith Laboratories). The apparent slight excess of iron in the unit cell composition may be due to the presence of some Fe²⁺ in the as-synthesized material or a small amount of extraframework iron.

The as-synthesized FeAPO-5 was characterized by powder X-ray diffraction (XRD), FT-IR spectroscopy, and scanning electron microscopy (SEM). The XRD data was obtained using a Scintag XDS 2000 X-ray diffractometer and Cu K α radiation. FT-IR spectra were obtained from KBr pellets using a Nicolet Avatar spectrophotometer. Scanning electron micrographs (SEM) were taken on a Phillips XL 30 series SEM.

Thin Film Preparation. The FeAPO-5 targets for laser ablation were prepared by pressing a free-standing 2.5 cm pellet of the as-synthesized molecular sieve. This target was then mounted in a controlled-atmosphere chamber as previously described.² A Lumonics HyperEX-400 excimer laser was used to generate a 248 nm (KrF*) 14 ns pulse with a repetition rate of 10 Hz. The laser energy was measured using a Scientech pyroelectric head (Model 380402) and found to range from 55 to 125 mJ/pulse. A computer-controlled rastering mirror (Oriol) was used to reflect the laser beam 90° and raster the beam across the target material. A focusing lens was used to decrease the spot size of the laser beam to 0.001 cm². The substrate was a 500 Å TiN-coated silicon wafer (Texas Instruments, Inc) which served as one of the electrodes for our parallel plate capacitor previously described.⁶ The TiN substrate was positioned ~2.5 cm away from and at an angle of ~40° below the target. Typical film deposition conditions were as follows: laser power density, 100–200 MW/cm²; substrate temperature of 300–320 °C; and a background oxygen pressure of 250–300 mTorr, which resulted in a deposition rate of ~33 nm/min.

Posthydrothermal Treatment. Posthydrothermal treatment of the laser-deposited FeAPO-5 films was carried out by conventional gel and vapor phase transfer methods. In the case of the gel method, an FeAPO-5 synthesis mixture was prepared as described above and transferred to a 23 mL autoclave. The laser-deposited FeAPO-5 film was positioned in the autoclave containing the FeAPO-5 gel at an angle of ~60° with the laser-deposited FeAPO-5 film facing down to minimize material depositing from the gel. The films were then heated at 150 °C for 0.75–1.5 h. After hydrothermal treatment, the films were washed with deionized water and air-dried. Crystallinity and film thickness were determined by powder X-ray diffraction and scanning electron microscopy, respectively.

The vapor phase transfer method involves treating the laser-deposited FeAPO-5 films under nonsynthesis conditions. In this case, 3.5 mL of 85% H₃PO₄ were added to 9.13 mL of deionized H₂O with stirring. The acid solution was combined with 8.7 mL of triethylamine (TEA) and ~6–6.5 mL of this mixture was transferred into a 40 mL Teflon-lined stainless steel autoclave. The laser-deposited FeAPO-5 film was then placed (face up) on a Pyrex pedestal ~6.5 cm above the solution. The autoclave was sealed and heated at 150 °C for 18–24 h. The reorganized film was washed with deionized water and air-dried. The crystallinity and film thickness were determined by powder X-ray diffraction (XRD) and scanning electron microscopy (SEM), respectively.

Sensor Measurements. Capacitors were fabricated from the pulsed laser deposition of FeAPO-5 material on 0.75 cm² TiN-coated silicon wafer after calcination at 400 °C. The TiN served as one electrode and the other electrode was generated on the top of the FeAPO-5 film by vapor deposition of ~200 nm of a Au/Pd contact through a shadow mask using a Denton Desk Lab II sputter coater. The area of the Au/Pd electrode used in all capacitance measurements was 0.184 mm².

Capacitance measurements were made using a custom probe station equipped with an environmental chamber. The probe station consisted of a microscope over the environmental chamber used to position the probe tips on the capacitor and a series of gas manifolds and flow meters used to introduce different gases. Capacitance data were collected using a Wayne Kerr Precision component analyzer 6425B controlled using Labview software (National Instruments). The voltage

could be varied from 0 to 1.0 V. The ac frequency of the capacitor was varied from 20 to 500 Hz.

During gas sensor measurements the FeAPO-5-based device was placed into the environmental chamber of the probe station and purged with dry N₂ at a flow rate of 30 mL/min for 5 min in order to establish the background capacitance. Further purging did not alter the baseline, which was in the picofarad range for all sensors studied. Once a background capacitance was obtained, the sensor could then be exposed to different gases using the same flow rate and purge time.

The leakage current was determined by plotting current vs voltage with the voltage range set equal to that of the capacitance measurements being made (0–0.3 V). The breakdown voltage was determined by scanning the voltage from 0 to 1 V and observing a significant increase in the current. The gases used in the experiments were as follows: 99.999% purity N₂, 99.998% purity CO₂, 98% CO, 100 ppm CO in a 99.998% purity N₂ balance, and 100 ppm NH₃ in a 99.998% purity N₂ balance.

Responses to water are reported in terms of absolute humidity calculated by using the following equations:²⁷ saturation vapor pressure, $E_s(\text{mbars}) = 6.11 \times 10^{(7.5 \times T/(237.7 + T))}$, where T = temperature (in °C); actual vapor pressure, $E(\text{mbars}) = E_s \times (\%RH/100)$, where %RH is percent relative humidity; dewpoint temperature, $T_{dc}(\text{°C}) = [-430.22 + 237.7 \times \ln(E)]/[-\ln(E) + 19.8]$, absolute humidity, $D(\text{kg/m}^3) = (E \times 100)/[(T_{dc} + 273.15) \times 461.5]$.

Results and Discussion

Thin Film Preparation. The parallel plate capacitive type chemical sensor requires a thin, continuous dielectric film since capacitance is inversely proportional to the distance between the electrodes. An optimum thickness for the molecular sieve film that appears to provide a reasonable capacitance change without a significant leakage current is in the range of 250–400 nm. Pulsed laser ablation is a viable method for the deposition of uniform continuous films of molecular sieves in this thickness range.^{2–9} Well-adhered films derived from FeAPO-5 were deposited at a rate of ~33 nm/min.

The bulk FeAPO-5 is composed of clusters of rod-shaped crystals as shown in the SEM of Figure 2a. A free-standing pellet (Figure 2b) was made by a mechanical press, which causes some fragmentation of crystals; however, this has little or no impact on the ablation process. After this FeAPO-5 target was irradiated, there was a clear transformation of the pellet surface to give a pitted almost amorphous appearance (Figure 2c). Therefore, all laser ablation experiments were carried out using a fresh target and the laser beam was always exposed to a new surface. Irradiation of the FeAPO-5 target under 300 mTorr of O₂ produced a blue-colored plume of FeAPO-5 particles. These fragments then deposited on the heated TiN surface. Figure 3a shows the SEM of a laser-deposited FeAPO-5 film having a film thickness of ~400 nm. Close inspection of the film reveals a continuous film composed of tightly packed nanoparticles. The surface view shown in Figure 3b reveals the surface to be composed of small spherulike particles with an average particle size <1 μm. This is the result of the laser conditions used during deposition experiments, which result in splashing.²⁸ Upon using a lower laser power (< ~60 mJ/pulse),

(27) Ahrens, C. D. *Meteorology Today*; West Publishing: St. Paul, MN, 1991.

(28) Chrissy, D. B.; Hubler, G. K. *Pulsed Laser Deposition of Thin Films*; John Wiley and Sons: New York, 1994.

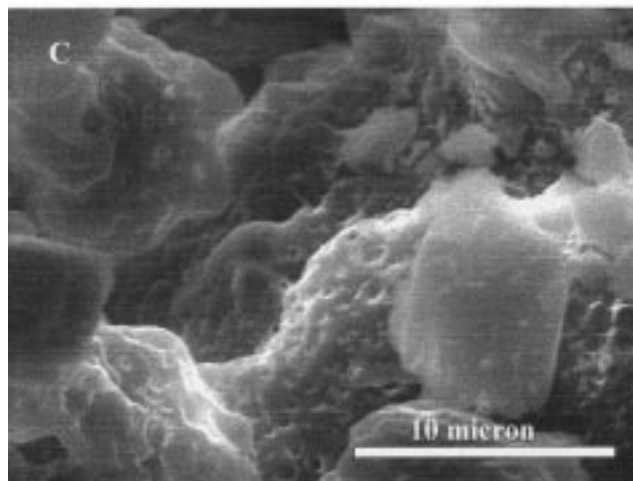
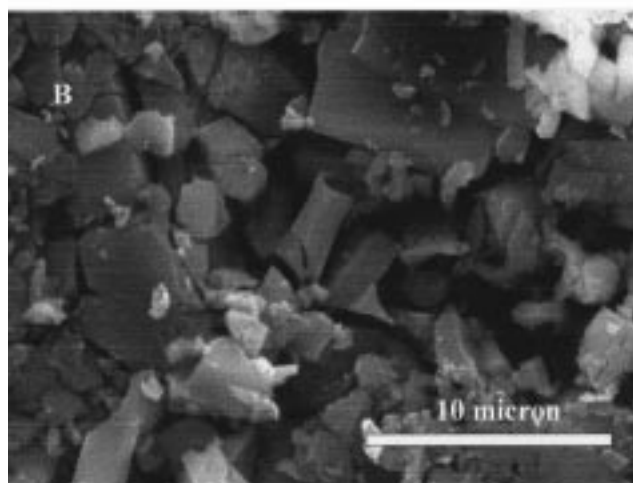
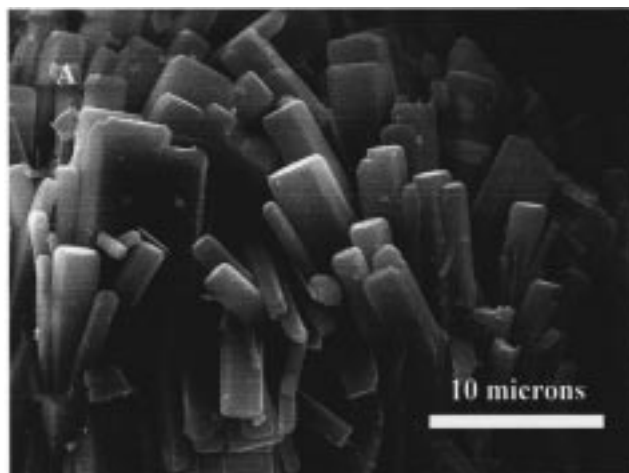


Figure 2. SEM of FeAPO-5 (A) as-synthesized bulk, (B) target pellet before ablation, and (C) target pellet after ablation.

splashing and particle size can be reduced; however, a longer ablation time would be necessary in order to produce a well-adhered film.

Figure 4a shows an FT-IR spectrum of the FeAPO-5 bulk material showing a large band at $\sim 1115\text{ cm}^{-1}$ characteristic of the asymmetric Al-O stretch. The band at $\sim 750\text{ cm}^{-1}$ could be assigned to the symmetric stretching mode while the bands at around 560 and 630 cm^{-1} were assigned to the double ring modes. The band at $\sim 476\text{ cm}^{-1}$ was assigned to the internal T-O bending

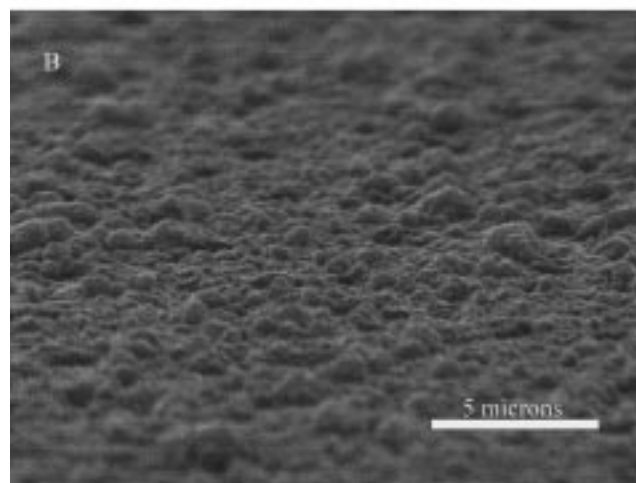
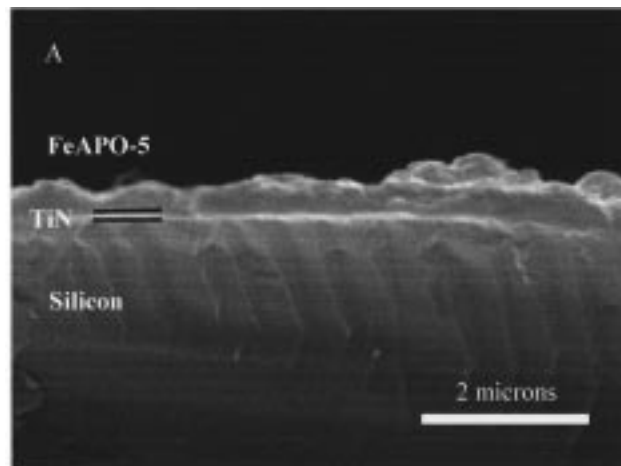


Figure 3. SEM cross section view of (A) laser-deposited FeAPO-5 on TiN and (B) surface view.

mode.²⁹ In contrast, Figure 4b shows the FT-IR spectra of FeAPO-5 ablated onto a KBr pellet, which indicates the presence of a noncrystalline FeAPO-5-derived film due to the lack of the more structure sensitive bands. The bands for the asymmetric and the T-O bending mode at ~ 1143 and 470 cm^{-1} respectively, of the ablated FeAPO-5 material correspond to those bands found in amorphous aluminum phosphate mixtures we have prepared as well as the band in the 950 cm^{-1} region which may indicate the presence of defect sites. In contrast, the bands found in the region between 700 and 740 cm^{-1} in the ablated FeAPO-5 sample were not present in amorphous aluminum phosphate but were present in the bulk FeAPO-5 material. This may reflect FeAPO-5 fragments of an unknown nature which can be reorganized quickly to a crystalline film. For our sensor applications these laser-deposited films had thicknesses in a usable range, however, the surface was much too uneven for use as a parallel plate capacitor device. Additionally, it has been shown²⁻⁹ that it was necessary for the molecular sieve film to exhibit partial crystallinity in order to obtain reasonable sensor responses. Therefore, these PLD FeAPO-5 films needed to be treated further.

In previous work we found that the crystallinity of the laser-deposited AlPO_4 and MeAPO films could be

(29) Rabo, J. A. *ACS Monogr.* 1976, 171, 81.

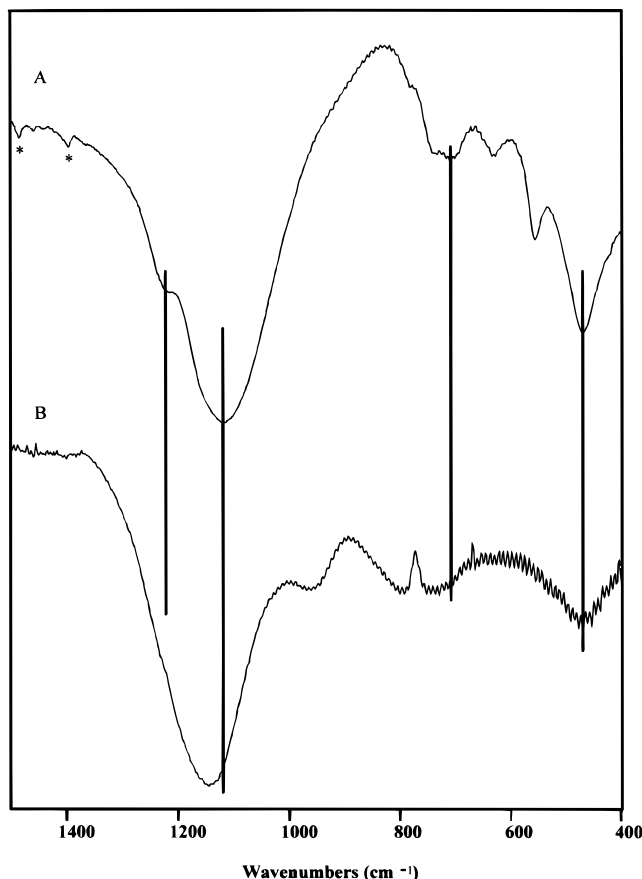


Figure 4. FT-IR spectra of (A) as-synthesized FeAPO-5 and (B) laser-deposited FeAPO-5 film; * denotes bands due to organic template.

improved by a brief hydrothermal treatment.²⁻⁸ For example in the case of laser-deposited AlPO₄-5 films the crystallinity of the film could be achieved using a hydrothermal treatment of 2 h at 150 °C without an increase in film thickness. These are conditions that do not crystallize AlPO₄-5 in solution. Similar treatments were applied to VAPO, MAPO, and MnAPO systems and found to reorganize the laser-deposited surface without increasing the thickness of the film. The laser-deposited film therefore appeared to exhibit a memory effect and possibly contained fragments that acted as nucleation sites that make this type of reorganization facile. The hydrothermal treatments of the FeAPO-5 films were initiated by using an FeAPO-5 gel having the molar ratios 1.0:0.1:0.9:1.0:40 TEAOH:Fe₂O₃:Al₂O₃:P₂O₅:H₂O.²⁶ The films were placed into the gel at an angle of ~60° and hydrothermally treated for only 1.0 h. After the elapsed time the films were removed from the gel mixture. Figure 5 shows the SEM of an FeAPO-5 film hydrothermally treated for 1 h which has grown to a thickness of ~4 μm from a starting film thickness of only 400 nm. X-ray analysis indicated the presence of a crystalline film shown in Figure 6b compared with a bulk sample of FeAPO-5 in Figure 6a. The XRD pattern indicative of FeAPO-5 was evident from the presence of the 100, 110, 200, 210, 002, and 211 reflections. X-ray analysis of the gel mixture did not show any crystalline FeAPO-5, which is consistent with other MeAPO systems studied, suggesting that the laser-deposited films can act as nucleation sites for film growth.²⁻⁸ Although the 1 h hydrothermal treatment

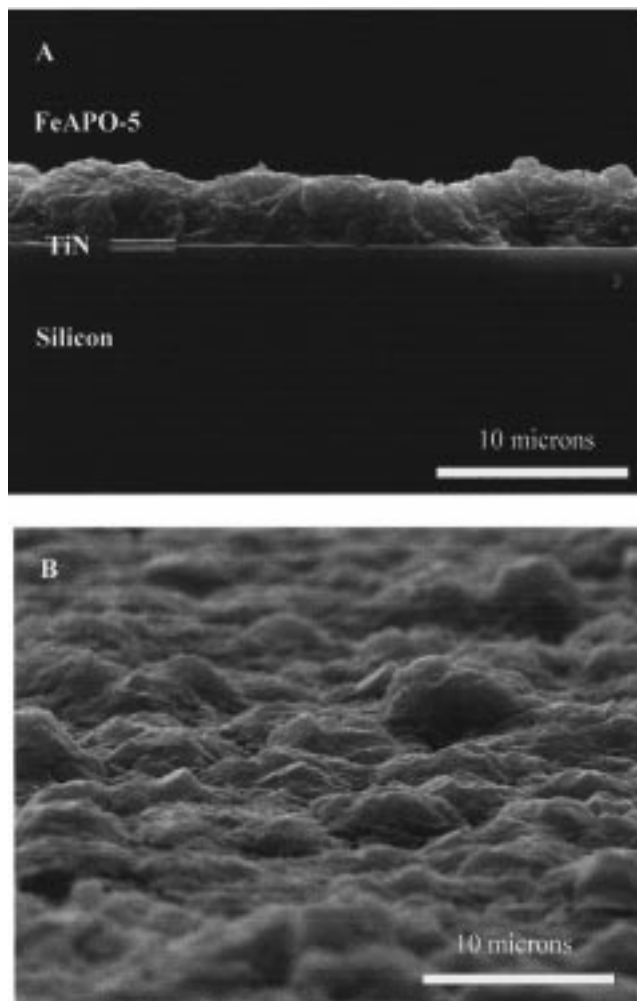


Figure 5. SEM cross section view of (A) FeAPO-5 film after a 1 h hydrothermal treatment and (B) a surface view.

yielded a crystalline film, the thickness was much too large for use as a capacitor. Recall that a thin, smooth continuous film is essential for a parallel plate capacitive type chemical sensor. It appears that the desired film thickness for these capacitive type devices is in the range of 250–400 nm, which will give the optimum capacitance change while also limiting the amount of leakage current.²⁻⁸ Since it appeared that the FeAPO-5 films crystallized much faster than the previously studied MeAPO-5 thin films under similar hydrothermal conditions, it was decided to treat the FeAPO-5 laser deposited films for shorter amounts of time. We found that after 0.5 h no crystallinity was present; however, nearly 100% crystallinity was observed between 45 min and 1 h of hydrothermal treatments. The crystallinity obtained during those times was comparable to that shown in the diffraction pattern in Figure 6. SEM images (not shown) once again revealed films that were all greater than 1 μm in thickness having surface morphologies that were continuous but rough.

It appeared that reorganization of the PLD FeAPO-5 films in a synthesis gel yields continuous crystalline films, but it was too difficult to control the film thickness. In contrast to the other AlPO₄ and MeAPO systems studied in Table 1, FeAPO-5 crystallizes so fast that the submicron films needed for the sensor do not seem readily accessible. To obtain crystalline films in the nanometer range, the hydrothermal treatment

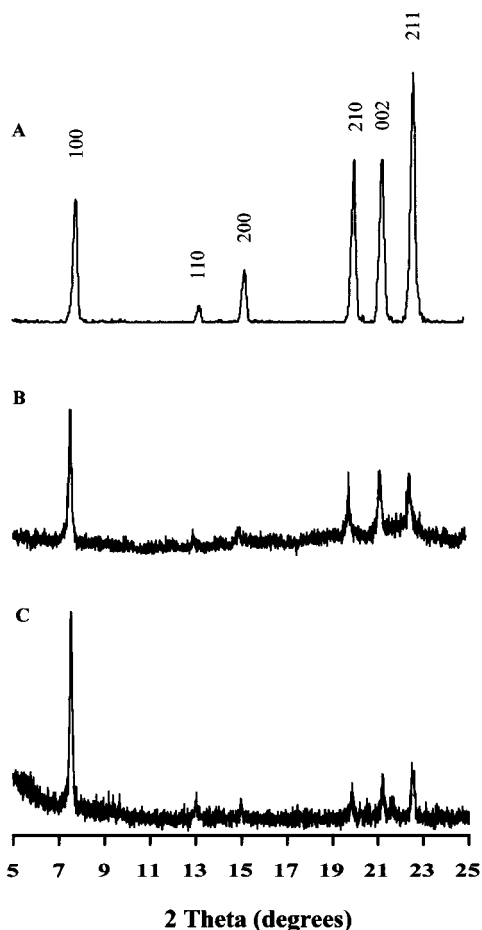


Figure 6. X-ray diffraction patterns of (A) as-synthesized FeAPO-5, (B) FeAPO-5 film hydrothermally treated for 1 h, and (C) an FeAPO-5 film vapor phase treated for 24 h.

should involve reagents that allow for the laser-deposited films to reorganize but not grow. We were encouraged by a synthetic procedure referred to as the vapor phase transport method recently reported for several zeolites. Xu et al.³⁰ first reported that the aluminosilicate ZSM-5 could be crystallized from an amorphous dry gel by exposing the solid to vapors of a triethylamine (TEA), ethylenediamine (EDA), and water mixture. The list of zeolites synthesized by this method has been expanded to include analcime, mordenite, and ferrierite.^{30–38} Additionally, some of these zeolites have been fabricated into supported membranes using this technique.^{30–38}

Although the vapor phase transport method does not appear to have ever been applied to aluminophosphate

molecular sieves, we attempted this procedure by utilizing a large 40 mL autoclave in which was placed a Pyrex pedestal on which the laser-deposited film was supported face up. Initially the vapor phase transport experiments involved only water in the bottom of the autoclave with exposure of the film to water vapor at 150 °C for 1–4 days. After the elapsed time no crystallinity in the FeAPO-5 films was observed by XRD. Next a mixture of water and triethylamine (9.13 mL of H₂O and 8.7 mL of triethylamine) was used in an attempt to reorganize the film over a period of 1–4 days at 150 °C. Perhaps not surprisingly there was no effect on the PLD films under these basic conditions, since the phosphate-based molecular sieves generally crystallize under acidic conditions (pH 3–5).¹ Therefore, H₃PO₄ was added to the mixture with a molar ratio of 1.0:1.0:40 TEA:P₂O₅:H₂O. After 24 h at 150 °C the laser-deposited FeAPO-5 film had reorganized into a partially crystalline film, as shown in Figure 6c. A comparison with the bulk FeAPO-5 XRD pattern in Figure 6a shows the presence of a pure phase partially crystalline FeAPO-5 film. The (100) reflection is the most intense peak with medium intensity reflections (210, 002, 211) and weak reflections (110, 200). The diminished intensities of the higher angle reflections with respect to the (100) reflection is different for the FeAPO-5 film compared with the bulk FeAPO-5. Bein et al.³⁹ reported partially oriented crystal growth of AlPO₄-5 crystals on an organophosphate film. We have also observed oriented film growth of for MAPO-39⁴⁰ as well as zeolite UTD-1 from PLD films.⁴¹ However, if the PLD FeAPO-5 films exhibit any preferred orientation, it is limited.

Figure 7a shows the SEM of the cross section of a reorganized FeAPO-5 film. The molecular sieve film is approximately 300 nm thick compared with the 400 nm laser deposited film in Figure 3. Apparently there was some dissolution of the debris from splashing during the vapor phase treatment into a slightly thinner film with a smooth surface. A top view in Figure 7b shows a smooth continuous film surface. Treating the PLD films for longer than 24 h using the acid/template reaction mixture above resulted in the formation of FeAPO-34 as an impurity along with FeAPO-5, as determined by XRD. Normally under these synthesis conditions FeAPO-34 does not appear as a product until after 7 days of heating.^{26,44} Decreasing the ratio of amine template to water or acid did not result in film reorganization. Holding the acid and water content constant to the original mixture but increasing the concentration of the template by a factor of 1.5 did yield a crystalline film comparable to the above films, but further template addition resulted in no improvement in crystallinity. Longer vapor phase treatments did not further enhance the crystallinity of the FeAPO-5 films even after 5 days of treatment. However, the morphology of these films treated for more than 24 h revealed a rough surface, as shown in Figure 8. Since the parallel plate capacitor configuration requires a uniform thin film, it would

(30) Xu, W.; Dong, J.; Li, J.; Li, J.; Wu, F. *J. Chem. Soc., Chem. Commun.* **1990**, 755.

(31) Kim, M. H.; Li, H. X.; Davis, M. E. *Micropor. Mater.* **1993**, *1*, 219.

(32) Nishiyama, N.; Ueyama, K.; Matsukata, M. *J. Chem. Soc., Chem. Commun.* **1995**, 1967.

(33) Matsukata, M.; Nishiyama, N.; Ueyama, K. *J. Chem. Soc., Chem. Commun.* **1994**, 339.

(34) Nishiyama, N.; Ueyama, K.; Matsukata, M. *Micropor. Mater.* **1996**, *7*, 299.

(35) Matsukata, M.; Nishiyama, N.; Ueyama, K. *Stud. Surf. Sci. Catal.* **1994**, *84*, 1183.

(36) Nishiyama, N.; Matsufuji, T.; Ueyama, K.; Matsukata, M. *Micropor. Mater.* **1997**, *12*, 293.

(37) Nishiyama, N.; Ueyama, K.; Matsukata, M. *Ceramics Processing* **1997**, *43*, 2724.

(38) Nishiyama, N.; Ueyama, K.; Matsukata, M. *Stud. Surf. Sci. Catal.* **1997**, *105*, 2195.

(39) Feng, S.; Bein, T. *Science* **1994**, *265*, 1839.

(40) Washmon, L.; Balkus, K. J., Jr. Manuscript in preparation.

(41) Balkus, K. J., Jr.; Muñoz, T., Jr.; Gimon-Kinsel, M. E. *Chem Mater.* **1998**, *2*, 464.

(42) Guochuan, F.; Di, T. *Stud. Surf. Sci. Catal.* **1989**, 281.

(43) Ojo, A. F.; Dwyer, J.; Parish, R. V. *Stud. Surf. Sci. Catal.* **1989**, 227.

(44) Park, J. W.; Chon, H. *J. Catalysis* **1992**, *133*, 159.

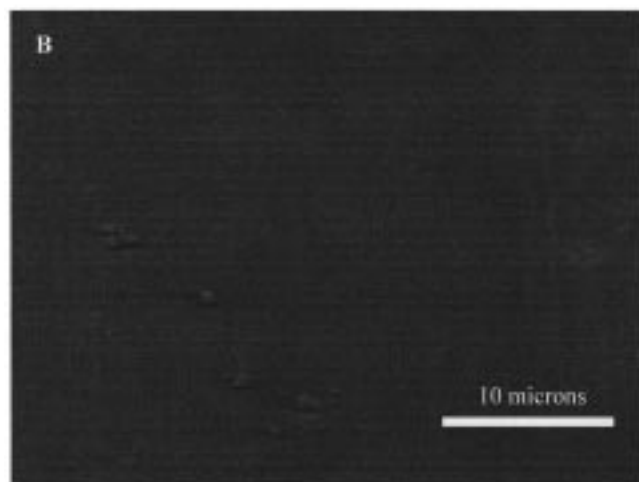
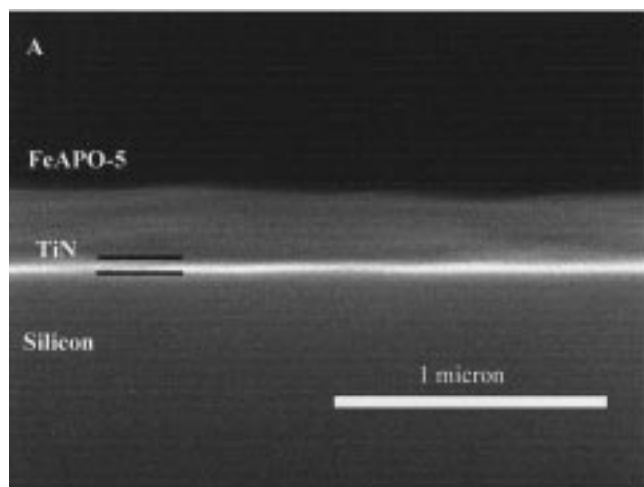


Figure 7. SEM cross section view of (A) an FeAPO-5 film vapor phase treated for 1 h and (B) a surface view.

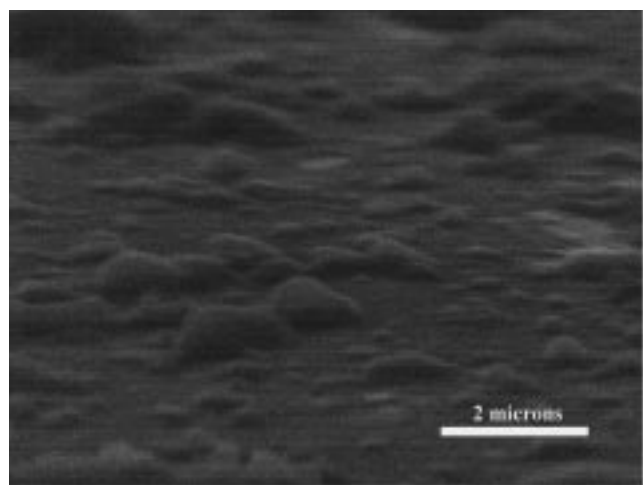


Figure 8. SEM surface view of FeAPO-5 film vapor phase treated for 24 h with 1.5 times more TEOH template.

appear the 24 h treatment is optimal. The exact nature of the vapor under these optimal conditions is uncertain, but the water must be transporting a certain amount of acid and template to the film. Although further perturbations to the vapor phase transport method for FeAPO-5 merits further investigation, the quality of the films was obtained deemed sufficient to fabricate sensors. It should also be pointed out that the intensity of

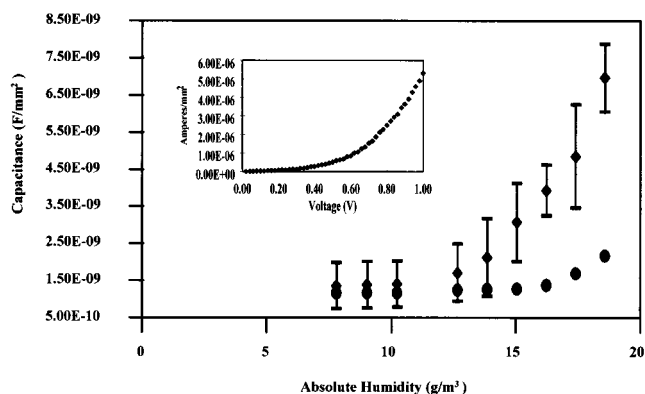


Figure 9. Plot of capacitance/area (F/mm^2) versus absolute humidity (g/m^3) with inset of current/area (amperes/ mm^2) versus voltage (V), from an average of (◆) five calcined films and (●) five uncalcined films.

the film XRD pattern (Figure 2c) relative to the bulk (Figure 2a) may reflect the thin nature of the deposit (~ 300 nm). Even if there are some amorphous regions, they apparently do not affect the sensor properties (vide infra).

Sensor Studies. FeAPO-5 films obtained by the vapor phase transport method were calcined at $400^\circ C$ for 6–8 h in order to decompose any organic template occluded in the pores. A shadow mask was used to pattern a Au/Pd alloy by sputtering. The thickness of the Au/Pd electrodes was ~ 200 Å. This means that the adsorption of the analytes must occur around the Au/Pd electrode. Evaluation of the FeAPO-5 sensor was conducted in an environmental probe chamber, where electrodes were positioned on a Au/Pd pad as well as an exposed surface of TiN. The capacitance was then monitored at an applied voltage of 0.3 V at an ac frequency of 100 Hz. The breakdown voltage was typically observed to be at around 1 V, which was evident by a sharp increase in leakage current. Various gases were introduced through a series of gas manifolds and flow meters into the environmental chamber for sensor measurements.

FeAPO-5 extends the series of isostructural $AlPO_4$ molecular sieves having AFI topology that have been studied as capacitive type sensors,^{2–8} where in general CO and CO_2 caused the greatest capacitance change while N_2 and H_2O gave the smallest change. The incorporation of framework metal ions such as Co^{2+} into the $AlPO_4$ -5 framework results in a greater response to CO .⁸ It was anticipated that the analogous iron molecular sieve FeAPO-5 would exhibit similar selectivity. Exposure of the FeAPO-5 films to N_2 , CO_2 , CO, NH_3 , and H_2O resulted in capacitance changes quite different from other MeAPO-5-based sensors. The FeAPO-5 sensor did not exhibit capacitance changes when exposed to CO or CO_2 relative to N_2 . Surprisingly, the FeAPO-5 sensor was quite sensitive to water, resulting in large capacitance changes.

Figure 9 shows a plot of average capacitance/ mm^2 versus absolute humidity at room temperature for five different FeAPO-5 devices all having a film thickness of ~ 300 nm. The leakage current for these devices is on the order of 10^{-8} A/ mm^2 . It has been shown^{2–8} that to obtain the greatest response in a capacitive type sensor a very thin film is desired, since capacitance is

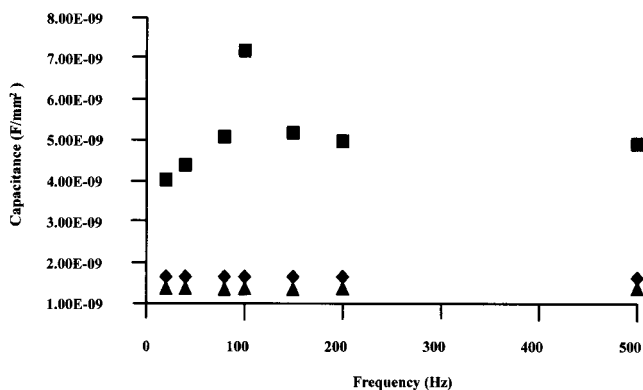


Figure 10. Plot of capacitance/area (F/mm^2) versus frequency (Hz), (◆) $19 \text{ g}/\text{m}^3$, (●) $14 \text{ g}/\text{m}^3$, (▲) $10 \text{ g}/\text{m}^3$, for a 300 nm FeAPO-5 film.

inversely proportional to the thickness of the dielectric. However, leakage current will increase as the film becomes thin. As a result, there exists a balance between obtaining a thin film and minimizing the leakage current in a device. We have determined that a film thickness between 250 and 400 nm is preferred for our capacitive type sensor.²⁻⁸ As one can see from the plot in Figure 9, the humidity responses of the FeAPO-5 devices are nonlinear. At the lower absolute humidity levels between 8 and $10 \text{ g}/\text{m}^3$ the capacitance response is fairly flat. As the humidity is increased from 12 to $25 \text{ g}/\text{m}^3$ there is a sharp increase in capacitance. In contrast, when a crystalline but uncalcined film containing template was tested at various humidity levels, the response was much lower than a crystalline calcined film. This is consistent with a significant portion of the calcined FeAPO-5 film response arising from adsorption of water into the pores. This response arises from the dipolar interactions that occur with the oxide surface and the energy of interaction water has with the internal pore species.^{5,10}

Figure 10 shows a plot of capacitance/ mm^2 versus frequency at absolute humidity levels of 10, 14, and $19 \text{ g}/\text{m}^3$ humidity for an FeAPO-5 sensor (300 nm thick film). The capacitance response for the absolute humidity levels at 10 and $14 \text{ g}/\text{m}^3$ did not vary over the range of frequencies tested. At a humidity level of $19 \text{ g}/\text{m}^3$, the capacitance response seemed to be dependent on the frequency used, showing trend of increasing response as the frequency was increased from 20 to 100 Hz, where the capacitance response appeared to reach a maximum. As the frequency was increased further, there is a leveling off of the capacitance response beginning at about 150 Hz. It has been reported that at low frequencies a material may exhibit a high relative permittivity ϵ_s , whereas at higher frequencies the relative permittivity reaches a low value along with a drop in capacitance. Such a reduction in relative permittivity with increasing frequency may be from dielectric dispersion; however, 150 Hz is too low for this phenomenon. At a humidity of $19 \text{ g}/\text{m}^3$ water may condense in the pores and on the surface, which may contribute to these results.

In comparison to the other AlPO_4 and MeAPO devices tested using, N_2 , CO, CO_2 , and H_2O , it is clear that FeAPO-5 behaves much differently. One would expect FeAPO-5 to respond at the very least like AlPO_4 -5 when exposed to CO or CO_2 ; however, this is not the case. One

difference is the presence of about one Fe atom per unit cell. As a result, a blank experiment was run to see if the observed responses with FeAPO-5 were the result of any extraframework surface species. A pure sample of AlPO_4 -5 was mixed with $\sim 2\%$ Fe_2O_3 by weight, which should model extraframework iron. This mixture was then ablated onto TiN using the same conditions used for FeAPO-5. The laser-deposited films were then vapor phase treated as above; however, a crystalline film was not obtained. In separate experiments we have also shown that the vapor phase method did not work for AlPO_4 -5, CoAPO-5, or MAPO-39 compositions. Nonetheless to be consistent, the films which had film thicknesses of $\sim 300 \text{ nm}$ were calcined and made into sensors. When sensor measurements were attempted using these devices, no measurable responses were recorded.

The iron in the as-synthesized FeAPO-5 has been shown to exist in the framework as a mixture of Fe^{2+} and Fe^{3+} ions;⁴²⁻⁴⁶ however, during calcination all the iron is converted to Fe^{3+} . ESR studies have revealed that calcined FeAPO-5 has two major signals, $g = 2.0$ and 4.3.⁴²⁻⁴⁶ The signal at $g = 4.3$ was attributed to octahedral Fe^{3+} ions in lattice defect sites which are coordinated both to bridging lattice oxygen and to terminal oxygen atoms caused by bond breakage and ligand coordination. The signal at $g = 2.0$ is attributed to Fe^{3+} ions in framework lattice sites coordinating to four intact lattice oxygen bridges and two ligand molecules in the pore. It cannot, however, be excluded that some extraframework Fe^{3+} either in cationic sites or oxide clusters contribute to this signal.⁴²⁻⁴⁶

Although simply admixed Fe_2O_3 does not promote the molecular sieve crystallization and does not result in a working sensor, one cannot exclude the presence of oxide clusters in the pores. If the effective pore is reduced, then adsorption of molecules such as CO (kinetic diameter 3.8 Å) and CO_2 (kinetic diameter 3.3 Å) might be hindered compared to that of the smaller water molecules (kinetic diameter 2.65 Å). A size exclusion effect of this type was observed in the small pore AlPO_4 -H3 system ($3.5 \times 3.7 \text{ Å}$).²⁻⁶ In this case, water is readily adsorbed, causing a capacitance response; however, CO and CO_2 do not cause a change in capacitance. Additionally, if the FeAPO-5 selectivity were simply due to pore blockage, one would expect the calcination to have a reverse effect and the response should vary between different films; however, this does not appear to be the case. The enhanced response of FeAPO-5 to humidity may also be explained by coordination of at least two water molecules to Fe^{3+} in addition to surface adsorption.

In conducting the humidity experiments it was discovered that the FeAPO-5 films also exhibit a quick response to the moisture in breath. Figure 11 shows a response from a 300 nm FeAPO-5 film where capacitance/ mm^2 is plotted versus time (s) using a voltage set at 0.3 V with a frequency of 100 Hz at 26°C . This plot shows a quick response time on the order of $\sim 2 \text{ s}$ that is reproducible and recoverable to seven different instances where the author breathed over the sensor. The

(45) Catana, G.; Pelgrims, J.; Schoonheydt, R. A. *Zeolites* **1995**, *15*, 475.

(46) Brückner, A.; Lohse, U.; Mehner, H. *Micropor. Mesopor. Mater.* **1998**, *20*, 207.

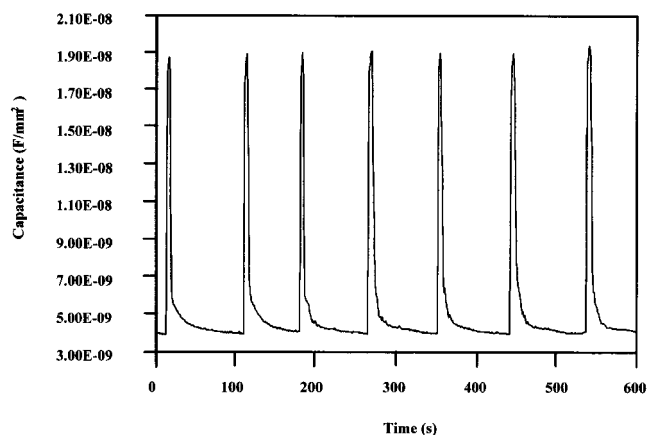


Figure 11. Plot of capacitance/area (F/mm^2) versus time (s) for an FeAPO-5 sensor response to even breaths by mouth.

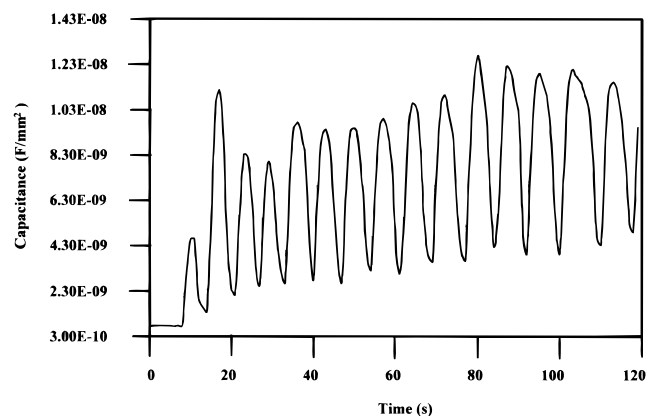


Figure 12. Plot of capacitance/area (F/mm^2) versus time (s) for an FeAPO-5 sensor response to nasal breathing without hesitation.

experiment was conducted by placing the sensor in the environmental probe chamber without a nitrogen flow and lightly breathing by mouth on the device at a distance of ~ 15 cm away. These are conditions similar to that recently reported by Stucky et al.⁴⁷ in which a humidity sensor based on C_{60} responded to the moisture in human breath. In the FeAPO-5 case, once the capacitance recovered to a background (~ 35 s) the process was repeated. One can see in Figure 11 that after the exposure to the moisture in a typical breath, a significant capacitance change is registered. Practical application would not allow a 35 s recovery time; therefore, the experiment was conducted using normal breathing through the nose. Figure 12 shows the response from a ~ 300 nm film of FeAPO-5 where capacitance/ mm^2 versus time (s) is plotted for this normal breathing experiment. The response time is on the order of ~ 2 s with a partial recovery ($\sim 80\%$) time of about 3 s between breaths. During normal breathing a recovery of $\sim 80\%$ is still possible. In contrast to other humidity sensors that also work on the principle of either capacitance or impedance,⁴⁸ these FeAPO-5 sensor response times are fast. For example, a range of 1 s for a cellulose acetate capacitive sensor to 10 min for a LiCl + glass fiber sheet impedance device has been

reported.⁴⁸ The detection limits required of most commercial sensors ideally is 1% relative humidity up to 100% relative humidity. The magnitude in the change in capacitance of some commercial sensors compared to our device is also quite different. For example, in the cellulose acetate capacitive sensor, the ΔC between 0 and 100% relative humidity was only ~ 15 pF. Similarly a polyimide-based capacitor had a ΔC of only 30 pF between 20 and 90% relative humidity. In contrast, our humidity sensor exhibits a ΔC of ~ 5700 pF between 30 and 75% relative humidity, which indicates a greater sensitivity to moisture for our sensor at high humidity levels.⁴⁵ Due to the nature of our experimental setup, ~ 8 g/m^3 absolute humidity (30% relative humidity) is the lower limit that was achieved during humidity measurements. The plot in Figure 9 from the FeAPO-5 device exhibits an exponential response that if one extrapolates the curve back to 0 g/m^3 absolute humidity, the capacitance would measure 1.08×10^{-9} F/mm^2 . Therefore the ΔC for our sensor between 0 and 8 g/m^3 absolute humidity (0–30% relative humidity) would be 284 pF. This change in capacitance is much greater than the capacitance changes observed for the above capacitors in the 0–100% relative humidity range. At 10% humidity a ΔC of ~ 6 pF is predicted; therefore an FeAPO-5 sensor may also be well-suited for low humidity detection. A molecular sieve sensor of this type might have some interesting applications particularly for monitoring respiration. For example, Ma et al.⁴⁹ developed an air flow humidity sensor in order to monitor neonatal infant respiration. This device is based on a polyimide capacitance type humidity sensor. In this capacitor the top electrode is made up of concentric rings in order to facilitate water absorption, a problem not inherent to the FeAPO-5 sensor. The response of the polymer sensor is in the low picofarad range with a change in capacitance of ~ 8 pF between 30 and 80% relative humidity, probably due to the thick polyimide film (1.38 μm). In our system, where a much thinner film is used, a higher capacitance change might be observed over the range of humidity exhaled by an infant which varies from 70 to 95% humidity.⁴⁹

Conclusions

Thin films of FeAPO-5 molecular sieve were successfully deposited on TiN by pulsed laser ablation followed by a vapor phase treatment. This appears to be the first example where an aluminophosphate type molecular sieve has been crystallized using a vapor phase transport method. Capacitive type chemical sensors based on laser-deposited FeAPO-5 films appear to be selective for the detection of water. As a result of this high response to humidity, we anticipate many applications will emerge, including a respiration monitoring device.

Acknowledgment. We thank the Texas Advanced Technology Program and the National Science Foundation for financial support of the research. We also thank Dr. Mary Gimón-Kinsel for helpful discussions.

CM9805222

(47) Saab, A. P.; Laub, M.; Srdanov, V. I.; Stucky, G. D. *Adv. Mater.* **1998**, *10*, 462.

(48) Ishihara, T. *Selective Electrode Rev.* **1992**, *14*, 1.

(49) Ma, Y.; Ma, S.; Wang, T.; Fang, W. *Sensors Actuators A* **1995**, *49*, 47.